

A multi-D model for Raman amplification

by M. Colin and T. Colin,
Université de Bordeaux
IMB, INRIA Bordeaux Sud Ouest, Team MC2
351 cours de la libération, 33405 Talence cedex, France.

mcolin@math.u-bordeaux1.fr
colin@math.u-bordeaux1.fr

Abstract : In this paper, we continue the study of the Raman amplification in plasmas that we initiated in [7] and [8]. We point out that the Raman instability gives rise to three components. The first one is collinear to the incident laser pulse and counter propagates. In 2-D, the two other ones make a non-zero angle with the initial pulse and propagate forward. Furthermore they are symmetric with respect to the direction of propagation of the incident pulse. We construct a non-linear system taking into account all these components and perform some 2-D numerical simulations.

1 Introduction

1.1 Presentation and statement of the results.

The interaction of powerful laser pulse with a plasma gives rise to several complex multiscale phenomena. It is of great interest since it occurs in the laboratory simulations of nuclear fusion (NIF, Laser Mega Joule). One of the key mechanism is the Raman instability that can be coupled with Landau damping (see [1]). In [7] and [8], we have initiated a systematic mathematical study of the Raman amplification process in plasma by justifying nonlinear models in 1-D and 2-D. There is a huge physical literature dedicated to the subject, see for example [3], [9] and [12]. A lot of conclusions and qualitative results are obtained. From the mathematical point of view, no real multi-D coupled system (i.e. involving coupled several directions of propagation) is available since the paraxial approximation is always used. The aim of this paper is to construct (as rigorously as possible) such a quasilinear system. There exists other works related to propagation of beams in transverse directions see [14, 15] for example. In [13], the authors elaborate a formalism for continuous spectrum related to Raman amplification. At the time being, we are not able to use this formalism

AMS classification scheme number: 35Q55, 35Q60, 78A60, 74S20

in the present work. In this paper, we focus on the 2D problem. The 3D one seems to be more difficult to handle since it involves a cone of diffraction that would have to be treated by the formalism of [13], but we are not able to embed a model in this framework. Finally, we refer to [11] for the mathematical theory of quasilinear Schrödinger equations.

These models rely on the propagation of three kind of waves : the initial laser pulse (K_0, ω_0) , the Raman component (K_R, ω_R) and the electron-plasma wave $(K_1, \omega_{pe} + \omega_1)$ where K and ω stand respectively for the wave vector and the frequency and ω_{pe} is the electron-plasma frequency. In order to be efficient, the interaction has to be a three waves mixing that is the data must satisfy the following relationships :

- The dispersion relation for electromagnetic waves

$$\omega_0^2 = \omega_{pe}^2 + c^2|K_0|^2, \quad (1.1)$$

$$\omega_R^2 = \omega_{pe}^2 + c^2|K_R|^2, \quad (1.2)$$

where c is the velocity of light in the vacuum.

- The dispersion relation for electron-plasma waves

$$(\omega_{pe} + \omega_1)^2 = \omega_{pe}^2 + v_{th}^2|K_1|^2, \quad (1.3)$$

where v_{th} denotes the thermal velocity of the electrons (see section 2.1 for its value).

- The three waves resonance conditions

$$\omega_0 = \omega_{pe} + \omega_R + \omega_1, \quad (1.4)$$

$$K_0 = K_R + K_1. \quad (1.5)$$

Note that ω_0 , ω_R , c v_{th} and K_0 are fixed. Therefore, we have 4 unknowns for 4 Equations (1.2)-(1.5). Even in 2-D, one can find solutions of this system such that K_1 , K_R and K_0 are collinear. This corresponds to the solution used in [7], [8]. The aim of this paper is to provide a more general study in order to understand the influence of the geometry. We solve (1.1) – (1.5) numerically and show that there exists infinitely many solutions in the plane. We compute the amplification rates associated to these solutions and show that the backward solution has a maximum amplification rate when it is collinear to the initial pulse, while the most two amplified forward directions make a non-zero angle with the laser pulse and are symmetric with respect to the direction of propagation of the incident pulse (see Section 2 and Section 3).

In Section 4, we introduce a non-linear model taking into account both direction of propagations. First, denote by A_0 the incident laser field, K_0 and ω_0 the associated wave vector and frequency, A_{R_1} the backscattered Raman component, K_{R_1} and ω_{R_1} the associated wave vector and frequency, A_{R_2} the forward Raman component, K_{R_2} and ω_{R_2} the associated wave vector and frequency, and finally $A_{R_2^s}$ the second forward Raman component, $K_{R_2^s}$ and $\omega_{R_2^s}$ the associated wave vector and frequency. We denote by $E_{||}$ the longitudinal part of the electric field (see (2.16)). We assume that K_0 is collinear to the

x -axis and then K_{R_2} and $K_{R_2^s}$ are symmetric with respect to the x -axis. p is the low-frequency variation of the density of electrons. Furthermore, we put

$$K_0 = \begin{pmatrix} k_0 \\ 0 \end{pmatrix}, K_{R_1} = \begin{pmatrix} k_{R_1} \\ \ell_{R_1} \end{pmatrix}, K_{R_2} = \begin{pmatrix} k_{R_2} \\ \ell_{R_2} \end{pmatrix}, K_{R_2^s} = \begin{pmatrix} k_{R_2^s} \\ \ell_{R_2^s} \end{pmatrix},$$

$$\theta_{1,1} = K_{1,1} \cdot X - \omega_{1,1}t, \theta_{1,2} = K_{1,2} \cdot X - \omega_{1,2}t, \theta_{1,2^s} = K_{1,2^s} \cdot X - \omega_{1,2^s}t.$$

The variables $\theta_{1,1}$, $\theta_{1,2}$ and $\theta_{1,2^s}$ represent the phase mismatch between the electron-plasma waves and the three Raman components. They are defined precisely in (4.1). Using as usual $\frac{1}{k_0}$ (resp. $\frac{1}{\omega_0}$) as length (resp. time) scale, the system reads in a nondimensional form

$$i\left(\partial_t + \frac{c^2 k_0^2}{\omega_0^2} \partial_x\right) A_0 + \left(\frac{c^2 k_0^2}{2\omega_0^2} \Delta - \frac{c^4 k_0^4}{2\omega_0^4} \partial_x^2\right) A_0 = \frac{\omega_{pe}^2}{2\omega_0^2} p A_0 \quad (1.6)$$

$$- \nabla \cdot E_{||} \left(A_{R_1} e^{-i\theta_{1,1}} \frac{k_{R_1}}{|K_{R_1}|} + \alpha (A_{R_2} e^{-i\theta_{1,2}} + A_{R_2^s} e^{-i\theta_{1,2^s}}) \frac{k_{R_2}}{|K_{R_2}|} \right),$$

$$i\left(\partial_t + \frac{c^2 k_0}{\omega_{R_1} \omega_0} K_{R_1} \cdot \nabla\right) A_{R_1} + \frac{1}{2\omega_{R_1} \omega_0} \left(c^2 k_0^2 \Delta - \frac{c^4 k_0^2}{\omega_{R_1}^2} (K_{R_1} \cdot \nabla)^2 \right) A_{R_1}$$

$$= \frac{\omega_{pe}^2}{2\omega_0 \omega_{R_1}} p A_{R_1} - \nabla \cdot E_{||}^* A_0 e^{i\theta_{1,1}} \frac{k_{R_1}}{|K_{R_1}|}, \quad (1.7)$$

$$i\left(\partial_t + \frac{c^2 k_0}{\omega_{R_2} \omega_0} K_{R_2} \cdot \nabla\right) A_{R_2} + \frac{1}{2\omega_{R_2} \omega_0} \left(c^2 k_0^2 \Delta - \frac{c^4 k_0^2}{\omega_{R_2}^2} (K_{R_2} \cdot \nabla)^2 \right) A_{R_2}$$

$$= \frac{\omega_{pe}^2}{2\omega_0 \omega_{R_2}} p A_{R_2} - \alpha \nabla \cdot E_{||}^* A_0 e^{i\theta_{1,2}} \frac{k_{R_2}}{|K_{R_2}|}, \quad (1.8)$$

$$i\left(\partial_t + \frac{c^2 k_0}{\omega_{R_2} \omega_0} K_{R_2^s} \cdot \nabla\right) A_{R_2^s} + \frac{1}{2\omega_{R_2} \omega_0} \left(c^2 k_0^2 \Delta - \frac{c^4 k_0^2}{\omega_{R_2}^2} (K_{R_2^s} \cdot \nabla)^2 \right) A_{R_2^s}$$

$$= \frac{\omega_{pe}^2}{2\omega_0 \omega_{R_2}} p A_{R_2^s} - \alpha \nabla \cdot E_{||}^* A_0 e^{i\theta_{1,2^s}} \frac{k_{R_2^s}}{|K_{R_2^s}|}, \quad (1.9)$$

$$i\partial_t E_{||} + \frac{v_{th}^2 k_0^2}{2\omega_{pe} \omega_0} \Delta E_{||} = \frac{\omega_{pe}}{2\omega_0} p E_{||} + \nabla \cdot \left(A_0 A_{R_1}^* e^{i\theta_{1,1}} \frac{k_{R_1}}{|K_{R_1}|} \right.$$

$$\left. + \alpha (A_0 A_{R_2}^* e^{i\theta_{1,2}} + A_0 A_{R_2^s}^* e^{i\theta_{1,2^s}}) \frac{k_{R_2}}{|K_{R_2}|} \right), \quad (1.10)$$

$$\left(\partial_t^2 - c_s^2 \Delta\right) p = \frac{4m_e}{m_i} \frac{\omega_0 \omega_{R_1}}{\omega_{pe}^2} \Delta \left(|E_{||}|^2 + \frac{\omega_{pe}}{\omega_0} |A_0|^2 + \frac{\omega_{pe}}{\omega_{R_1}} |A_{R_1}|^2 \right.$$

$$\left. + \frac{\omega_{pe}}{\omega_{R_2}} (|A_{R_2}|^2 + |A_{R_2^s}|^2) \right), \quad (1.11)$$

where $\alpha = \sqrt{\frac{\omega_{R_1}}{\omega_{R_2}}}$. It will be shown later that $k_{R_2^s} = k_{R_2}$ and $|K_{R_2^s}| = |K_{R_2}|$. The constants c , c_s , m_e and m_i are respectively the velocity of light in vacuum, the acoustic velocity, the electron's and ion's mass. Note that we could consider separately the systems involving respectively the backward and forward scattered waves. But since they are coupled through (1.6)-(1.11), we have to consider the whole system for a complete description of the phenomena. The methods of [7] applies and one gets the following result.

Existence result : Let $s > \frac{d}{2} + 3$, $(a_0, a_{R_1}, a_{R_2}, a_{R_2^s}, e_0) \in (H^{s+2}(\mathbb{R}^d))^{5d}$, $p_0 \in H^{s+1}(\mathbb{R}^d)$ and $p_1 \in H^s(\mathbb{R}^d)$. There exists $T > 0$ and a unique maximal solution $(A_0, A_{R_1}, A_{R_2}, A_{R_2^s}, E_{||}, p)$ to (1.6) – (1.11) such that

$$(A_0, A_{R_1}, A_{R_2}, A_{R_2^s}, E_{||}) \in \left(C([0, T[; H^{s+2}) \right)^{5d},$$

$$p \in C([0, T[; H^{s+1}) \cap C^1([0, T[; H^s),$$

with initial value

$$(A_0, A_{R_1}, A_{R_2}, A_{R_2^s}, E_{||})(0) = (a_0, a_{R_1}, a_{R_2}, a_{R_2^s}, e_0)$$

$$p(0) = p_0, \quad \partial_t p(0) = p_1.$$

In Section 5, we perform some numerical simulations in order to illustrate the phenomena and to emphasize the new directions of propagation.

1.2 The method.

As said before, the Raman amplification is essentially a three waves mixing phenomena. As a consequence, we introduce three waves vectors K_0 , K_R and K_1 and three frequencies ω_0 , ω_R and ω_1 satisfying

$$\begin{cases} K_0 = K_R + K_1, & (1.12) \end{cases}$$

$$\begin{cases} \omega_0 = \omega_R + (\omega_{pe} + \omega_1), & (1.13) \end{cases}$$

such that (K_0, ω_0) , (K_R, ω_R) satisfy the dispersion relation for electromagnetic waves (2.15) namely $\omega^2 = \omega_{pe}^2 + c^2|K|^2$ and $(K_1, \omega_1 + \omega_{pe})$ satisfies that for electron-plasma waves $\omega^2 = \omega_{pe}^2 + v_{th}^2|K|^2$. We choose the form $(K_1, \omega_1 + \omega_{pe})$ for the electron-plasma waves because of the relative shapes of the two curves represented in Figure 1.

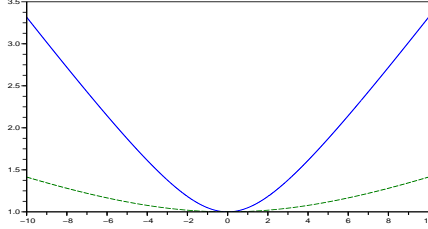


Figure 1: Plot of the first part of the dispersion relations (2.14) (dashed line) and (2.15) (solid line) with $\omega_{pe}^2 = 1$, $c^2 = 1$ and $v_{th}^2 = 0.01$. The plot corresponds to ω as a function of $|K|$.

Indeed, whatever the value of (K_0, ω_0) , $\omega_1 + \omega_{pe}$ will be close to ω_{pe} so that $\omega_1 \ll \omega_{pe}$. However, in this configuration, K_1 can take a continuous range of values.

The weakly non-linear theory consists in decomposing the different fields F into three components

$$F = F_0 e^{i(K_0 \cdot X - \omega_0 t)} + F_R e^{i(K_R \cdot X - \omega_R t)} + F_e e^{-i\omega_e t} + \text{c.c.}$$

We then plug this decomposition into Maxwell's system and collect the different coefficients of the oscillatory terms in $e^{-i\omega_0 t}$, $e^{-i\omega_R t}$ and $e^{-i\omega_{pe} t}$. We deal only with the oscillations in time (which is not the case when one has to derive the paraxial approximation in optics for example) since, as we emphasized before, K_1 can take a continuous range of values. This lead to the following result :

1) For the linear part, each of the component satisfies a Schrödinger-type equation with the suitable group velocity and dispersion terms.

2) For the non-linear part, we keep only the resonant terms (with respect to the time oscillations). Therefore, some phase mismatch terms appear under the form $e^{i(K_1 \cdot X - \omega_1 t)}$. These terms describe two phenomena: the first one is the fact that K_1 can take a continuous range of values and the second one corresponds to the fact that the relationship $\omega_0 = \omega_R + \omega_{pe}$ is not true and that one has to add a corrective term $\omega_1 \ll \omega_{pe}$ in order to obtain the exact relationship (1.13).

We have used this strategy in [7], [8]. We would like to emphasize that it is a non-standard method and that it is not clear which framework could be used from the mathematical point of view in order to justify rigorously this expansion. For example, the work by Texier (see [16]) can not be adapted in this case because precisely of this three wave mixing phenomena.

The main contribution of this paper is to deal with the 2D situation. The equations describing the three-wave mixing have two curves of solutions. One of these curve corresponds to a backward solution, the other one to a forward

solution. The question is : how can we select two particular solutions (one backward, one forward)? The answer that we propose here is the following one. We derive a non-linear system starting from bifluid Euler-Maxwell system that describes the three wave interaction for any prescribed solution of the three wave mixing equations. From this system, as in [8], we compute an amplification rate thanks to a semi-classical analysis. At the beginning of the phenomena, the Raman components is growing exponentially before to reach a non-linear saturation regime. Therefore, only the solutions corresponding to the maximal amplification rate has a significant effect. Since two directions of propagation are involved (backward and forward), we look separately to both cases. The conclusion is the following one :

- for the backward component, the amplification rate reaches its maximum when this wave is collinear to the incident laser field,
- for the forward component, the situation is different since the amplification rate is maximum when the Raman component has a non-zero prescribed angle (depending on the different constants involved in the system). One has therefore to consider two components that are symmetric with respect to the direction of propagation of the incident laser field.

Note that in each situation, the amplification rate exhibits only one maximum. We then generalize the construction of the non-linear system to the case where several directions of propagation are involved. By non-linear effects, all these waves are coupled and this leads to System (1.6)-(1.11).

The 3-D case is completely open. Indeed, the same analysis can be performed concerning the amplification rate. Again the backward solution has a maximum amplification rate when it is aligned with the incident laser field. However, due to the invariance by rotations in the plane that is transverse to the direction of propagation of the laser, a continuous curve of solutions have the same maximal amplification rate for the forward component. Therefore, we would have to deal with a continuous family of component and to our knowledge, no mathematical framework is available in order to deal with the phase mismatch description in this context. In the work by Barraillh and Lannes ([13]) where the notion of continuous spectrum is introduced, the non-linear interactions are basically killed by the analysis except under very special geometrical assumptions on the dispersion relation that are not satisfied in our case.

2 Obtaining a 2-D Raman amplification system

2.1 The Euler-Maxwell system

As noticed in the introduction, the main drawback of the model developed in [7] is the fact that the Raman component and the incident laser field are collinear in the sense that the wave vectors are proportional (in opposite direction). The aim of this section is to get rid of this hypothesis. We will only sketch the computations that are very close to the ones done in [7]. We start from the

bifluid Euler-Maxwell system. The Euler equations are

$$(n_0 + n_e) (\partial_t v_e + v_e \cdot \nabla v_e) = -\frac{\gamma_e T_e}{m_e} \nabla n_e - \frac{e(n_0 + n_e)}{m_e} (E + \frac{1}{c} v_e \times B), \quad (2.1)$$

$$(n_0 + n_i) (\partial_t v_i + v_i \cdot \nabla v_i) = -\frac{\gamma_i T_i}{m_i} \nabla n_i + \frac{e(n_0 + n_i)}{m_i} (E + \frac{1}{c} v_i \times B), \quad (2.2)$$

$$\partial_t n_e + \nabla \cdot ((n_0 + n_e) v_e) = 0, \quad (2.3)$$

$$\partial_t n_i + \nabla \cdot ((n_0 + n_i) v_i) = 0. \quad (2.4)$$

The Maxwell system is written in terms of the electronic-magnetic fields for the study of the electron-plasma waves (Langmuir waves)

$$\partial_t B + c \nabla \times E = 0, \quad (2.5)$$

$$\partial_t E - c \nabla \times B = 4\pi e((n_0 + n_e) v_e - Z(n_0 + n_i) v_i), \quad (2.6)$$

while the formulation with magnetic potential, electric potential and electric field in the Lorentz gauge is used for the study of the electromagnetic waves (light)

$$\partial_t \psi = c \nabla \cdot A, \quad (2.7)$$

$$\partial_t A + c E = c \nabla \psi, \quad (2.8)$$

$$\partial_t E - c \nabla \times \nabla \times A = 4\pi e((n_0 + n_e) v_e - Z(n_0 + n_i) v_i), \quad (2.9)$$

where Z is the atomic number of the ions. We first perform a linear analysis of system (2.1) – (2.9) and compute the dispersion relations as well as the polarization conditions. Then using the time envelope approximation, we derive a quasilinear system describing the interaction.

2.2 Dispersion relations and polarization conditions.

Since the mass of the ions is much larger than that of the electrons (a ratio of at least 10^3), the velocity of the ions is smaller than that of the electrons. Therefore we can neglect the contribution of the ions in the current in (2.6) or (2.9). We then linearize System (2.1) – (2.9) around the steady state solution 0 and one gets

$$n_0 \partial_t v_e = -\frac{\gamma_e T_e}{m_e} \nabla n_e - \frac{en_0}{m_e} E, \quad (2.10)$$

$$\partial_t n_e + n_0 \nabla \cdot v_e = 0, \quad (2.11)$$

$$\partial_t B + c \nabla \times E = 0, \quad (2.12)$$

$$\partial_t E - c \nabla \times B = 4\pi en_0 v_e. \quad (2.13)$$

Note that the acoustic part concerning the ions is decoupled from the high-frequency part concerning the electrons and will be considered below. We look for plane wave solutions to (2.10) – (2.11) of the form $e^{i(K \cdot X - \omega t)}(v_e, n_e, B, E)$. Two kind of waves can propagate :

i) Longitudinal waves for which K is parallel to E (electron-plasma wave). They satisfy the dispersion relation

$$\omega^2 = \omega_{pe}^2 + v_{th}^2 |K|^2, \quad (2.14)$$

with

$$\omega_{pe}^2 = \frac{4\pi e^2 n_0}{m_e}, \quad v_{th}^2 = \sqrt{\frac{\gamma_e T_e}{m_e}}.$$

ii) Transverse waves for which K is orthogonal to E (electromagnetic waves). They obey the dispersion relation

$$\omega^2 = \omega_{pe}^2 + c^2 |K|^2. \quad (2.15)$$

Since for our applications, $v_{th} \ll c$, the shape of the graph of (2.14) or (2.15) are very different. Indeed, (2.14) is very flat near the origin compared to (2.15) (see Figure 1). Therefore, even if a precise couple (K_0, ω_0) is imposed for the incident laser field, we have to consider only the frequency ω_{pe} for the electron-plasma wave with a continuous range K of wave vectors. Therefore, the complete solution reads

$$\begin{pmatrix} B \\ E \\ v_e \\ n_e \end{pmatrix} = \begin{pmatrix} B_{||} \\ E_{||} \\ v_{e||} \\ n_{e||} \end{pmatrix} e^{-i\omega_{pe}t} + \sum_{j=1}^k \begin{pmatrix} B_{\perp}^j \\ E_{\perp}^j \\ v_{e\perp}^j \\ 0 \end{pmatrix} e^{i(K_j \cdot X - \omega_j t)} + c.c. \quad (2.16)$$

where $||$ corresponds to the longitudinal part and \perp corresponds to the transverse part. Furthermore, for all $1 \leq j \leq k$,

$$\omega_j^2 = \omega_{pe}^2 + c^2 |K_j|^2. \quad (2.17)$$

As usual $(B_{||}, E_{||}, v_{e||}, n_{e||})$ and $(B_{\perp}^j, E_{\perp}^j, v_{e\perp}^j)$ satisfy some polarization conditions that are obtained like in [7] by plugging plane waves in (2.10) – (2.13),

$$v_{e||} = -i \frac{\omega_{pe}}{4\pi e n_0} E_{||}, \quad B_{||} = 0, \quad n_{e||} = -\frac{1}{4\pi e} \nabla \cdot E_{||}.$$

For the transverse part, one writes $B_{\perp} = \nabla \times A_{\perp}$ and using the Maxwell system in the Lorentz gauge we get

$$-i\omega_j A_{\perp}^j + c E_{\perp}^j = 0, \quad (2.18)$$

$$-i\omega_j E_{\perp}^j + c K_j \times K_j \times A_{\perp}^j = 4\pi n_0 v_{e\perp}, \quad (2.19)$$

$$-i\omega_j v_{e\perp}^j = -\frac{e}{m_e} E_{\perp}^j. \quad (2.20)$$

Using (2.19) and (2.20), one obtains

$$-i\omega_j E_{\perp}^j + c K_j \times K_j \times A_{\perp}^j = -i \frac{4\pi e^2 n_0}{m_e \omega_j} E_{\perp}^j.$$

It follows that E_{\perp}^j is orthogonal to K_j and therefore so do A_{\perp}^j and $v_{e\perp}^j$. In a 2-D geometry, this leads to look for E_{\perp}^j , A_{\perp}^j and $v_{e\perp}^j$ under the form

$$(E_{\perp}^j, A_{\perp}^j, v_{e\perp}^j) \frac{K_j^{\perp}}{|K_j|}, \quad (2.21)$$

where $(E_{\perp}^j, A_{\perp}^j, v_{e\perp}^j)$ denote now scalar functions. Note that K_j^{\perp} is orthogonal to K_j in the plane defined by (K_0, K_R) . We do not deal with s-polarized waves. The polarization relations on these scalar fields read

$$v_{e\perp}^j = \frac{e}{m_e c} A_{\perp}^j, \quad E_{\perp}^j = i \frac{\omega_j}{c} A_{\perp}^j. \quad (2.22)$$

2.3 The weakly nonlinear theory.

We restrict ourself to the 2D case. Since we are interested in the Raman instability, we take $k = 2$ in (2.16) and write

$$\begin{aligned} \begin{pmatrix} B \\ E \\ v_e \\ n_e \end{pmatrix} &= \begin{pmatrix} 0 \\ E_{||} \\ v_{e||} \\ n_{e||} \end{pmatrix} e^{-i\omega_{pe}t} + \begin{pmatrix} B_0 \\ E_0 \\ v_{e0} \\ 0 \end{pmatrix} e^{i(K_0 \cdot X - \omega_0 t)} \\ &+ \begin{pmatrix} B_R \\ E_R \\ v_{eR} \\ 0 \end{pmatrix} e^{i(K_R \cdot X - \omega_R t)} + c.c., \end{aligned} \quad (2.23)$$

where the subscript 0 stands for the incident laser field and R for the Raman component. The purpose of the weakly non-linear theory is to propose a non-linear system that describes the three wave mixing phenomena. We recall here our general strategy explained in the introduction for the derivation of the coupled non-linear system. To this end, we introduce three wave vectors K_0 , K_R and K_1 and three frequencies ω_0 , ω_R and ω_1 satisfying

$$\begin{cases} K_0 = K_R + K_1, \\ \omega_0 = \omega_R + (\omega_{pe} + \omega_1), \end{cases} \quad (2.24)$$

$$(2.25)$$

such that (K_0, ω_0) , (K_R, ω_R) satisfy the dispersion relation for electromagnetic waves (2.15) namely $\omega^2 = \omega_{pe}^2 + c^2 |K|^2$ and $(K_1, \omega_1 + \omega_{pe})$ satisfies that for electron-plasma waves $\omega^2 = \omega_{pe}^2 + v_{th}^2 |K|^2$. The weakly non-linear theory consists in decomposing the different fields F into three components

$$F = F_0 e^{i(K_0 \cdot X - \omega_0 t)} + F_R e^{i(K_R \cdot X - \omega_R t)} + F_e e^{-i\omega_e t} + c.c.$$

We then plug this decomposition into Maxwell system and collect the different coefficients of the oscillatory terms in $e^{-i\omega_0 t}$, $e^{-i\omega_R t}$ and $e^{-i\omega_{pe} t}$. We deal only with the oscillations. As explained above, this leads to the following result :

the linear behavior of the waves is governed by Schrödinger-type equations. For the non-linear part, we perform a Fourier analysis in time keeping only the resonant terms. This analysis induces the presence of phase mismatch terms of the form $e^{i(K_1 \cdot X - \omega_1 t)}$ that come from the fact that a continuous range of values of K_1 are admissible and that the relationship $\omega_0 = \omega_R + \omega_{pe}$ is not exact but approximative in the way that $\omega_1 \ll \omega_{pe}$ (see (2.25)).

From now on, when we deal with a generic vector field, we use the bold character \mathbf{A} whereas the notation A denotes a scalar field.

• Equation on \mathbf{A}_0 and \mathbf{A}_R . The equations satisfied by each of the electromagnetic fields $(\mathbf{B}_0, \mathbf{E}_0, \mathbf{v}_{e0})$ and $(\mathbf{B}_R, \mathbf{E}_R, \mathbf{v}_{eR})$ are, using the vector potential \mathbf{A} ($\mathbf{A} = \mathbf{A}_0$ or \mathbf{A}_R)

$$\partial_t^2 \mathbf{A} - c^2 \Delta \mathbf{A} = -4\pi e c (n_0 + n_e) \mathbf{v}_e.$$

We now write

$$\mathbf{A} = \mathbf{A}_0 e^{i(K_0 \cdot X - \omega_0 t)} + \mathbf{A}_R e^{i(K_R \cdot X - \omega_R t)} + \text{c.c.},$$

and introduce the scalar components A_0 and A_R of \mathbf{A}_0 and \mathbf{A}_R with respect to K_0^\perp and K_R^\perp ,

$$A_0 = P_{K_0^\perp} \mathbf{A}_0, \quad A_R = P_{K_R^\perp} \mathbf{A}_R,$$

where $P_{K_0^\perp}$ and $P_{K_R^\perp}$ are the orthogonal projector onto K_0^\perp and K_R^\perp . Collecting the terms depending on $e^{i(K_0 \cdot X - \omega_0 t)}$ (resp. $e^{i(K_R \cdot X - \omega_R t)}$) and applying $P_{K_0^\perp}$ (resp. $P_{K_R^\perp}$) leads to, as in [7], the following equations

$$\begin{aligned} & i \left(\partial_t + \frac{c^2}{\omega_0} K_0 \cdot \nabla \right) A_0 + \frac{1}{2\omega_0} \left(c^2 \Delta - \frac{c^4}{\omega_0^2} (K_0 \cdot \nabla)^2 \right) A_0 \\ &= \frac{2\pi e^2}{\omega_0 m_e} p A_0 - \frac{e}{2\omega_0 m_e} (\nabla \cdot E_{||}) A_R e^{-i\theta_1} \frac{K_0 \cdot K_R}{|K_0| |K_R|}, \end{aligned} \quad (2.26)$$

$$\begin{aligned} & i \left(\partial_t + \frac{c^2}{\omega_R} K_R \cdot \nabla \right) A_R + \frac{1}{2\omega_R} \left(c^2 \Delta - \frac{c^4}{\omega_R^2} (K_R \cdot \nabla)^2 \right) A_R \\ &= \frac{2\pi e^2}{\omega_R m_e} p A_R - \frac{e}{2\omega_R m_e} (\nabla \cdot E_{||}^*) A_0 e^{i\theta_1} \frac{K_0 \cdot K_R}{|K_0| |K_R|}. \end{aligned} \quad (2.27)$$

We recall here that p denotes the low-frequency variation of the density of electrons.

• Equation on $\mathbf{E}_{||}$. The electron-plasma part is very similar to that of [7].

We describe briefly the procedure. Using (2.1), (2.5) and (2.6), one has

$$\begin{aligned}
\partial_t^2 \mathbf{E} + c^2 \nabla \times \nabla \times \mathbf{E} &= 4\pi e \partial_t \left((n_0 + n_e) \mathbf{v}_e \right) \\
&= 4\pi e \left((n_0 + n_e) \partial_t \mathbf{v}_e + \mathbf{v}_e \partial_t n_e \right) \\
&= 4\pi e \left(- (n_0 + n_e) \mathbf{v}_e \cdot \nabla \mathbf{v}_e - \frac{\gamma_e T_e}{m_e} \nabla n_e \right. \\
&\quad \left. - \frac{e(n_0 + n_e)}{m_e} \left(\mathbf{E} + \frac{1}{c} \mathbf{v}_e \times \mathbf{B} \right) - \mathbf{v}_e \nabla \cdot \left((n_0 + n_e) \mathbf{v}_e \right) \right).
\end{aligned}$$

Keeping only at most quadratic terms gives

$$\begin{aligned}
\partial_t^2 \mathbf{E} + c^2 \nabla \times \nabla \times \mathbf{E} &= 4\pi e \left(- n_0 \mathbf{v}_e \cdot \nabla \mathbf{v}_e - \frac{\gamma_e T_e}{m_e} \nabla n_e \right. \\
&\quad \left. - \frac{e(n_0 + n_e)}{m_e} \mathbf{E} - \frac{en_0}{cm_e} \mathbf{v}_e \times \mathbf{B} - n_0 \mathbf{v}_e \nabla \cdot \mathbf{v}_e \right).
\end{aligned}$$

Using

$$\mathbf{E} = \mathbf{E}_0 e^{i(K_0 \cdot X - \omega_0 t)} + \mathbf{E}_R e^{i(K_R \cdot X - \omega_R t)} + \mathbf{E}_{||} e^{-i\omega_{pe} t} + \text{c.c.},$$

and collecting the $e^{-i\omega_{pe} t}$ terms leads to

$$\begin{aligned}
&\partial_t^2 \mathbf{E}_{||} - 2i\omega_{pe} \partial_t \mathbf{E}_{||} + c^2 \nabla \times \nabla \times \mathbf{E}_{||} - \omega_{pe}^2 \mathbf{E}_{||} + \frac{4\pi e \gamma_e T_e}{m_e} \nabla n_e \\
&= \left\langle 4\pi e \left(- n_0 \mathbf{v}_e \cdot \nabla \mathbf{v}_e - \frac{e(n_0 + n_e)}{m_e} \mathbf{E} - \frac{en_0}{cm_e} \mathbf{v}_e \times \mathbf{B} - n_0 \mathbf{v}_e \nabla \cdot \mathbf{v}_e \right) \right\rangle_{\omega_{pe}},
\end{aligned}$$

where $\langle \cdot \rangle_{\omega_{pe}}$ denotes the coefficient of $e^{-i\omega_{pe} t}$ in the expansion. Using the polarization condition

$$n_{e||} = -\frac{1}{4\pi e} \nabla \cdot \mathbf{E}_{||},$$

and noticing that

$$\omega_{pe}^2 \mathbf{E}_{||} = \left\langle 4\pi e \frac{en_0}{m_e} \mathbf{E} \right\rangle_{\omega_{pe}},$$

we obtain

$$\begin{aligned}
&\partial_t^2 \mathbf{E}_{||} - 2i\omega_{pe} \partial_t \mathbf{E}_{||} + c^2 \nabla \times \nabla \times \mathbf{E}_{||} - v_{th}^2 \nabla \nabla \cdot \mathbf{E}_{||} \\
&= \left\langle 4\pi e \left(- n_0 \mathbf{v}_e \cdot \nabla \mathbf{v}_e - \frac{en_e}{m_e} \mathbf{E} - \frac{en_0}{cm_e} \mathbf{v}_e \times \mathbf{B} - n_0 \mathbf{v}_e \nabla \cdot \mathbf{v}_e \right) \right\rangle_{\omega_{pe}}.
\end{aligned}$$

The nonlinear resonant terms are given by

$$\begin{aligned}
\left\langle \mathbf{v}_e \cdot \nabla \mathbf{v}_e \right\rangle_{\omega_{pe}} &= \left(\mathbf{v}_0 \cdot \nabla \mathbf{v}_R^* + \mathbf{v}_R^* \cdot \nabla \mathbf{v}_0 \right) e^{i\theta_1} + \mathbf{v}_0 \cdot \mathbf{v}_R^* \nabla e^{i\theta_1}, \\
\left\langle n_e \mathbf{E} \right\rangle_{\omega_{pe}} &= p \mathbf{E}_{||}, \\
\left\langle \mathbf{v}_e \times \mathbf{B} \right\rangle_{\omega_{pe}} &= \left(\mathbf{v}_0 \times \mathbf{B}_R^* + \mathbf{v}_R^* \times \mathbf{B}_0 \right) e^{i\theta_1},
\end{aligned}$$

$$\left\langle \mathbf{v}_e \nabla \cdot \mathbf{v}_e \right\rangle_{\omega_{pe}} = \left(\mathbf{v}_0 \nabla \cdot \mathbf{v}_R^* + \mathbf{v}_R^* \nabla \cdot \mathbf{v}_0 \right) e^{i\theta_1},$$

since \mathbf{v}_0 and \mathbf{v}_R^* are orthogonal. But

$$\begin{aligned} \mathbf{B}_0 &= \nabla \times \mathbf{A}_0, \quad \mathbf{v}_0 = \frac{e}{m_e c} \mathbf{A}_0, \\ \mathbf{B}_R &= \nabla \times \mathbf{A}_R, \quad \mathbf{v}_R = \frac{e}{m_e c} \mathbf{A}_R, \end{aligned}$$

then, it follows that

$$\begin{aligned} &\left\langle -n_0 \mathbf{v}_e \cdot \nabla \mathbf{v}_e - \frac{en_0}{cm_e} \mathbf{v}_e \times \mathbf{B} - n_0 \mathbf{v}_e \nabla \cdot \mathbf{v}_e \right\rangle_{\omega_{pe}} \\ &= -\frac{e^2 n_0}{m_e^2 c^2} \left(\mathbf{A}_0 \cdot \nabla \mathbf{A}_R^* + \mathbf{A}_R^* \cdot \nabla \mathbf{A}_0 + \mathbf{A}_0 \cdot \mathbf{A}_R^* \nabla (i\theta_1) \right. \\ &\quad \left. + \mathbf{A}_0 \times \nabla \times \mathbf{A}_R^* + \mathbf{A}_R^* \times \nabla \times \mathbf{A}_0 + \mathbf{A}_0 \nabla \cdot \mathbf{A}_R^* + \mathbf{A}_R^* \nabla \cdot \mathbf{A}_0 \right) e^{i\theta_1} \\ &\approx -\frac{e^2 n_0}{m_e^2 c^2} \nabla \left(\mathbf{A}_0 \cdot \mathbf{A}_R^* e^{i\theta_1} \right), \end{aligned}$$

since at first order, one has $\nabla \cdot \mathbf{A}_0 = 0$ and $\nabla \cdot \mathbf{A}_R^* = 0$ and therefore for a weakly nonlinear analysis $\mathbf{A}_0 \nabla \cdot \mathbf{A}_R^* + \mathbf{A}_R^* \nabla \cdot \mathbf{A}_0$ can be neglected. Computing

$$\mathbf{A}_0 \cdot \mathbf{A}_R^* = A_0 A_R^* \frac{K_0 \cdot K_R}{|K_0| |K_R|},$$

and using the time envelope approximation $\partial_t^2 \mathbf{E}_{||} \ll \omega_{pe} \partial_t \mathbf{E}_{||}$, it follows that

$$\begin{aligned} &-2i\omega_{pe} \partial_t \mathbf{E}_{||} + c^2 \nabla \times \nabla \times \mathbf{E}_{||} - v_{th}^2 \nabla \nabla \cdot \mathbf{E}_{||} \\ &= -\frac{4\pi e^2}{m_e} p \mathbf{E}_{||} - \frac{4\pi e^3 n_0}{m_e^2 c^2} \nabla \left(A_0 A_R^* e^{i\theta_1} \frac{K_0 \cdot K_R}{|K_0| |K_R|} \right). \end{aligned}$$

The final equation reads

$$\begin{aligned} &i\partial_t \mathbf{E}_{||} + \frac{v_{th}^2}{2\omega_{pe}} \nabla \nabla \cdot \mathbf{E}_{||} - \frac{c^2}{2\omega_{pe}} \nabla \times \nabla \times \mathbf{E}_{||} \\ &= \frac{\omega_{pe}}{2n_0} p \mathbf{E}_{||} + \frac{e\omega_{pe}}{2m_e c^2} \nabla \left(A_0 A_R^* e^{i\theta_1} \frac{K_0 \cdot K_R}{|K_0| |K_R|} \right). \end{aligned} \quad (2.28)$$

• Equation on p . The acoustic part is the same as in [7]. It is obtained by the usual procedure starting from (2.2)-(2.4) and reads

$$\left(\partial_t^2 - c_s^2 \Delta \right) p = \frac{1}{4\pi m_i} \Delta \left(|\mathbf{E}_{||}|^2 + \frac{\omega_{pe}^2}{c^2} (|A_0|^2 + |A_R|^2) \right), \quad (2.29)$$

where

$$c_s^2 = \frac{\gamma_i T_i}{m_i} + \frac{\gamma_e T_e}{m_e}.$$

System (2.26) – (2.29) is the 2-D Raman interaction system. Note that in this case, the usual ponderomotive force in the right-hand-side of (2.29) is modified compared to the usual one (see [17])

3 The amplification rates and the most amplified directions.

3.1 Semi-classical asymptotic.

As in [8], we introduce a semi-classical limit of System (2.26) – (2.29) in order to obtain amplification rates. Following [8], we take $p = 0$ in order to focus on the three waves mixing phenomena. We rewrite (2.26) – (2.28) under the following way by introducing a small parameter ε that describes the order of magnitude of the inverse of the frequency of the waves. Therefore, the phase θ_1 can be written

$$\theta_1 = \frac{(K_1 \cdot X - \omega_1 t)}{\varepsilon},$$

where K_1 and ω_1 are dimensionless wave number and frequency. We perform a semi-classical expansion in the spirit of [6] to obtain

$$\begin{aligned} & i\left(\partial_t + \frac{c^2}{\omega_0} K_0 \cdot \nabla\right) A_0 + \frac{\varepsilon}{2\omega_0} \left(c^2 \Delta - \frac{c^4}{\omega_0^2} (K_0 \cdot \nabla)^2\right) A_0 \\ &= -\varepsilon \frac{e}{2\omega_0 m_e} (\nabla \cdot \mathbf{E}_{||}) A_R e^{-i\theta_1} \frac{K_0 \cdot K_R}{|K_0||K_R|}, \end{aligned} \quad (3.1)$$

$$\begin{aligned} & i\left(\partial_t + \frac{c^2}{\omega_R} K_R \cdot \nabla\right) A_R + \frac{\varepsilon}{2\omega_R} \left(c^2 \Delta - \frac{c^4}{\omega_R^2} (K_R \cdot \nabla)^2\right) A_R \\ &= -\varepsilon \frac{e}{2\omega_R m_e} (\nabla \cdot \mathbf{E}_{||}^*) A_0 e^{i\theta_1} \frac{K_0 \cdot K_R}{|K_0||K_R|}, \end{aligned} \quad (3.2)$$

$$\begin{aligned} & i\partial_t \mathbf{E}_{||} + \varepsilon \left(\frac{v_{th}^2}{2\omega_{pe}} \nabla \nabla \cdot \mathbf{E}_{||} - \frac{c^2}{2\omega_{pe}} \nabla \times \nabla \times \mathbf{E}_{||} \right) \\ &= \varepsilon \frac{e\omega_{pe}}{2m_e c^2} \nabla \left(A_0 A_R^* e^{i\theta_1} \frac{K_0 \cdot K_R}{|K_0||K_R|} \right). \end{aligned} \quad (3.3)$$

Note that, since the right-hand-side of (3.3) is a gradient, one has $\nabla \times \mathbf{E}_{||} = 0$. Then $\mathbf{E}_{||}$ is a gradient and then a straightforward calculation (see [7] for more details) gives, after applying succesively the operators $\nabla \cdot$ and $\nabla \Delta^{-1}$ on (3.3)

$$i\partial_t \mathbf{E}_{||} + \varepsilon \frac{v_{th}^2}{2\omega_{pe}} \Delta \mathbf{E}_{||} = \varepsilon \frac{e\omega_{pe}}{2m_e c^2} \nabla \left(A_0 A_R^* e^{i\theta_1} \frac{K_0 \cdot K_R}{|K_0||K_R|} \right). \quad (3.4)$$

Denoting $\mathbf{E}_{||} = \mathcal{E} e^{i\frac{(K_1 \cdot X - \omega_1 t)}{\varepsilon}}$ we obtain

$$\begin{aligned} & i\left(\partial_t + \frac{c^2}{\omega_0} K_0 \cdot \nabla\right) A_0 + \frac{\varepsilon}{2\omega_0} \left(c^2 \Delta - \frac{c^4}{\omega_0^2} (K_0 \cdot \nabla)^2\right) A_0 \\ &= -i \frac{e}{2\omega_0 m_e} K_1 \cdot \mathcal{E} A_R \frac{K_0 \cdot K_R}{|K_0||K_R|} - \varepsilon \frac{e}{2\omega_0 m_e} (\nabla \cdot \mathcal{E}) A_R \frac{K_0 \cdot K_R}{|K_0||K_R|}, \end{aligned} \quad (3.5)$$

$$\begin{aligned}
& i\left(\partial_t + \frac{c^2}{\omega_R} K_R \cdot \nabla\right) A_R + \frac{\varepsilon}{2\omega_R} \left(c^2 \Delta - \frac{c^4}{\omega_R^2} (K_R \cdot \nabla)^2\right) A_R \\
& = i \frac{e}{2\omega_R m_e} K_1 \cdot \mathcal{E}^* A_0 \frac{K_0 \cdot K_R}{|K_0||K_R|} - \varepsilon \frac{e}{2\omega_R m_e} (\nabla \cdot \mathcal{E}^*) A_0 \frac{K_0 \cdot K_R}{|K_0||K_R|}, \quad (3.6)
\end{aligned}$$

$$\begin{aligned}
& \left(i\partial_t + \frac{1}{\varepsilon} \left(\omega_1 - \frac{v_{th}^2}{2\omega_{pe}} |K_1|^2\right) + i \frac{v_{th}^2}{\omega_{pe}} K_1 \cdot \nabla\right) \mathcal{E} + \varepsilon \frac{v_{th}^2}{2\omega_{pe}} \Delta \mathcal{E} \\
& = i \frac{e\omega_{pe}}{2m_e c^2} \left(A_0 A_R^* \frac{K_0 \cdot K_R}{|K_0||K_R|}\right) K_1 + \varepsilon \frac{e\omega_{pe}}{2m_e c^2} \nabla \left(A_0 A_R^* \frac{K_0 \cdot K_R}{|K_0||K_R|}\right). \quad (3.7)
\end{aligned}$$

Now recall that the third wave $(\omega_{pe} + \omega_1, K_1)$ satisfies the dispersion relation (2.14)

$$(\omega_{pe} + \omega_1)^2 = \omega_{pe}^2 + v_{th}^2 |K_1|^2,$$

and thus a direct expansion gives

$$\omega_1 \approx \frac{v_{th}^2 |K_1|^2}{2\omega_{pe}}.$$

Then the equation (3.7) on \mathcal{E} reads

$$\begin{aligned}
i\left(\partial_t + \frac{v_{th}^2}{\omega_{pe}} K_1 \cdot \nabla\right) \mathcal{E} + \varepsilon \Delta \mathcal{E} & = i \frac{e\omega_{pe}}{2m_e c^2} \left(A_0 A_R^* \frac{K_0 \cdot K_R}{|K_0||K_R|}\right) K_1 \\
& + \varepsilon \frac{e\omega_{pe}}{2m_e c^2} \nabla \left(A_0 A_R^* \frac{K_0 \cdot K_R}{|K_0||K_R|}\right). \quad (3.8)
\end{aligned}$$

Finally, denoting by

$$f_0 = \frac{\omega_{pe}}{c} A_0, \quad f_R = \frac{\omega_{pe}}{c} A_R, \quad f = \frac{K_1 \cdot \mathcal{E}}{|K_1|},$$

Equations (3.5), (3.6) and (3.8) become at leading order with respect to ε

$$\left(\partial_t + \frac{c^2}{\omega_0} K_0 \cdot \nabla\right) f_0 = -\frac{e|K_1|}{2\omega_0 m_e} f f_R \cos(\theta), \quad (3.9)$$

$$\left(\partial_t + \frac{c^2}{\omega_R} K_R \cdot \nabla\right) f_R = \frac{e|K_1|}{2m_e \omega_R} f^* f_0 \cos(\theta), \quad (3.10)$$

$$\left(\partial_t + \frac{v_{th}^2}{\omega_{pe}} K_1 \cdot \nabla\right) f = \frac{e|K_1|}{2m_e \omega_{pe}} f_0 f_R^* \cos(\theta), \quad (3.11)$$

where θ denotes the angle between K_0 and K_R .

3.2 Amplification rates.

In order to point out the amplification rates, we study the stability of the trivial solution $(f_0, 0, 0)$ where f_0 is a constant. Applying the Fourier transform

in space on Equations (3.10) and (3.11), we obtain (we denote by \widehat{f} the Fourier transform of a function f)

$$\partial_t \widehat{f}_R + i \frac{c^2}{\omega_R} \xi \cdot K_R \widehat{f}_R = \frac{e|K_1|}{2m_e \omega_R} f_0 \widehat{f}^* \cos(\theta) \quad (3.12)$$

$$\partial_t \widehat{f}^* + i \frac{v_{th}^2}{\omega_{pe}} \xi \cdot K_1 \widehat{f}^* = \frac{e|K_1|}{2m_e \omega_{pe}} f_0^* \widehat{f}_R \cos(\theta) \quad (3.13)$$

In order to decouple Equations (3.12) and (3.13), we apply the operator $\partial_t + i \frac{v_{th}^2}{\omega_{pe}} \xi \cdot K_1$ on (3.12) to derive, using (3.13)

$$\begin{aligned} & \partial_t^2 \widehat{f}_R + i \left(\frac{v_{th}^2}{\omega_{pe}} K_1 + \frac{c^2}{\omega_R} K_R \right) \cdot \xi \partial_t \widehat{f}_R \\ & - \left(\frac{c^2 v_{th}^2}{\omega_{pe} \omega_R} (\xi \cdot K_1)(\xi \cdot K_R) + \frac{e^2 |K_1|^2 |f_0|^2 \cos^2(\theta)}{4m_e^2 \omega_R \omega_{pe}} \right) \widehat{f}_R = 0. \end{aligned} \quad (3.14)$$

The discriminant associated with Equation (3.14) is then equal to

$$\begin{aligned} \Delta &= - \left(\left(\frac{v_{th}^2}{\omega_{pe}} K_1 + \frac{c^2}{\omega_R} K_R \right) \cdot \xi \right)^2 + 4 \left(\frac{c^2 v_{th}^2}{\omega_{pe} \omega_R} (\xi \cdot K_1)(\xi \cdot K_R) + \frac{e^2 |K_1|^2 |f_0|^2 \cos^2(\theta)}{4m_e^2 \omega_R \omega_{pe}} \right) \\ &= 4 \frac{e^2 |K_1|^2 |f_0|^2 \cos^2(\theta)}{4m_e^2 \omega_R \omega_{pe}} - \left(\left(\frac{v_{th}^2}{\omega_{pe}} K_1 - \frac{c^2}{\omega_R} K_R \right) \cdot \xi \right)^2. \end{aligned} \quad (3.15)$$

It is obvious that (3.15) reaches its maximum for

$$\xi \cdot \left(\frac{v_{th}^2}{\omega_{pe}} K_1 - \frac{c^2}{\omega_R} K_R \right) = 0, \quad (3.16)$$

which means that the growth rate of the solutions of Equations (3.12) and (3.13) is maximal if ξ satisfies (3.16). The amplification rate is therefore proportional to

$$\beta = \frac{|K_1|}{\sqrt{\omega_R \omega_{pe}}} |\cos(\theta)|.$$

Recall that the incident field propagates along the x -axis and that

$$K_0 = \begin{pmatrix} k_0 \\ 0 \end{pmatrix}, \quad K_R = \begin{pmatrix} k_R \\ \ell_R \end{pmatrix}, \quad K_1 = \begin{pmatrix} k_1 \\ \ell_1 \end{pmatrix}.$$

and remark that we have $\ell_R = -\ell_1$. The dispersion relation (2.14) and (2.15) gives

$$\begin{cases} \omega_0^2 = \omega_{pe}^2 + k_0^2 c^2, \\ \omega_R^2 = \omega_{pe}^2 + (k_R^2 + \ell_R^2) c^2, \\ (\omega_{pe} + \omega_1)^2 = \omega_{pe}^2 + v_{th}^2 (k_1^2 + \ell_1^2). \end{cases} \quad (3.17)$$

We take ω_{pe} as unit for ω and $\frac{\omega_{pe}}{c}$ as unit for k . Introduce

$$\rho = \frac{v_{th}}{c} \ll 1,$$

then System (3.17) can be rewritten into

$$\begin{cases} \omega_0^2 = 1 + k_0^2, \\ \omega_R^2 = 1 + (k_R^2 + \ell_R^2), \\ (1 + \omega_1)^2 = 1 + \rho^2(k_1^2 + \ell_1^2). \end{cases} \quad (3.18)$$

The amplification rate β is given by

$$\beta = \frac{\sqrt{k_1^2 + \ell_1^2}}{\sqrt{1 + k_R^2 + \ell_1^2}} \frac{|k_R|}{\sqrt{k_R^2 + \ell_1^2}}. \quad (3.19)$$

For given k_0, ω_0 satisfying $\omega_0^2 = 1 + k_0^2$, we therefore need to find the maximum of $\beta(k_R, k_1, \ell_1)$ subject to the constraints

$$\omega_R^2 = 1 + (k_R^2 + \ell_R^2), \quad (1 + \omega_1)^2 = 1 + \rho^2(k_1^2 + \ell_1^2), \quad k_0 = k_R + k_1.$$

Replacing k_R by $k_0 - k_1$ in (3.19) gives

$$\beta = \frac{\sqrt{k_1^2 + \ell_1^2}}{\sqrt{1 + (k_0 - k_1)^2 + \ell_1^2}} \frac{|k_0 - k_1|}{\sqrt{(k_0 - k_1)^2 + \ell_1^2}}, \quad (3.20)$$

with

$$\sqrt{1 + k_0^2} = \sqrt{1 + (k_0 - k_1)^2 + \ell_1^2} + \sqrt{1 + \rho^2(k_1^2 + \ell_1^2)}. \quad (3.21)$$

Note that since $\omega_0 = 1 + \omega_R + \omega_1$ and $\omega_R \geq 0, \omega_1 \geq 0$, one has thanks to (3.18), $\omega_R \geq 1$ and therefore $\omega_0 \geq 2$, which is the dimensionless version of the well-known condition $\omega_{pe} \leq \frac{\omega_0}{2}$ for the existence of the backward Raman scattering.

3.3 Conclusions.

The above problem (3.20) – (3.21) is solved numerically. The conclusions are the following ones. For the backscattered component ($k < 0$), the maximum is reached for $\ell_1 = 0$. This means that the most amplified direction corresponds to the case where the Raman field is collinear to the incident laser field (see Figure 2, left picture).

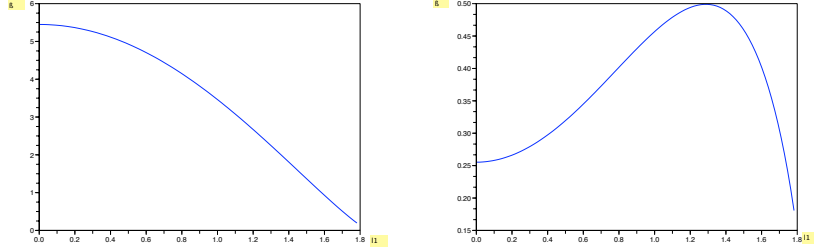


Figure 2: β with respect to ℓ_1 with $\rho = 0.01$ and respectively, from left to right, $k < 0$ and $k > 0$.

This model is used in [7]. For the forward component ($k > 0$), one can see in Figure 2 (right picture) that the maximum of β is reached for $\ell_1 \neq 0$. Therefore, the Raman field makes a non-zero angle with the incident laser pulse and gives rise to new direction of propagation.

For the sake of completeness, we now present some curves representing the amplification rate β with respect to ℓ_1 for different values of parameter ρ . In Figure 3, we take $\rho = 0.05$ and in Figure 4, $\rho = 0.001$. One can observe in Figure 3 and Figure 4 that the qualitative behaviour of β is the same than that observed in Figure 2.

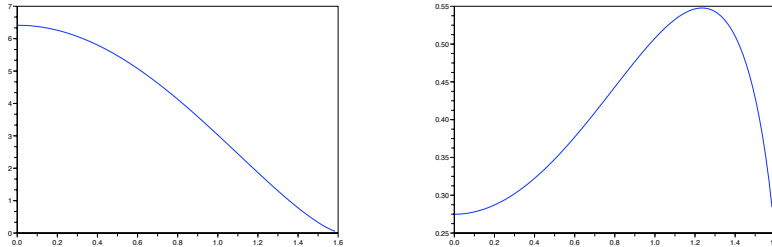


Figure 3: β with respect to ℓ_1 with $\rho = 0.05$ and respectively, from left to right, $k < 0$ and $k > 0$.

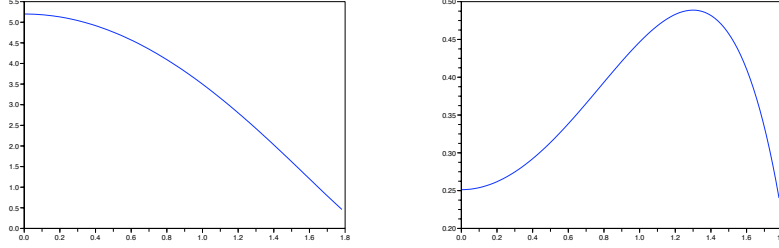


Figure 4: β with respect to ℓ_1 with $\rho = 0.001$ and respectively, from left to right, $k < 0$ and $k > 0$.

The next step is to take into account this new direction of propagation.

4 A complete model

4.1 Some basic tools

In order to describe the directions of propagation, one introduces the three wave vectors for the Raman component given by problem (3.20) – (3.21)

$$K_{R_1} = \begin{pmatrix} k_{R_1} \\ \ell_{R_1} \end{pmatrix}, K_{R_2} = \begin{pmatrix} k_{R_2} \\ \ell_{R_2} \end{pmatrix}, K_{R_2^s} = \begin{pmatrix} k_{R_2^s} \\ \ell_{R_2^s} \end{pmatrix},$$

satisfying

$$K_0 = K_{R_1} + K_{1,1} = K_{R_2} + K_{1,2} = K_{R_2^s} + K_{1,2^s},$$

that is

$$\begin{aligned} \begin{pmatrix} k_0 \\ 0 \end{pmatrix} &= \begin{pmatrix} k_{R_1} \\ \ell_{R_1} \end{pmatrix} + \begin{pmatrix} k_{1,1} \\ \ell_{1,1} \end{pmatrix}, \\ &= \begin{pmatrix} k_{R_2} \\ \ell_{R_2} \end{pmatrix} + \begin{pmatrix} k_{1,2} \\ \ell_{1,2} \end{pmatrix}, \\ &= \begin{pmatrix} k_{R_2^s} \\ \ell_{R_2^s} \end{pmatrix} + \begin{pmatrix} k_{1,2^s} \\ \ell_{1,2^s} \end{pmatrix}. \end{aligned}$$

We then introduce the Raman frequencies ω_{R_1} , ω_{R_2} and $\omega_{R_2^s}$ solution to

$$\begin{aligned} \omega_0 &= \omega_{pe} + \omega_{R_1} + \omega_{1,1}, \\ &= \omega_{pe} + \omega_{R_2} + \omega_{1,2}, \\ &= \omega_{pe} + \omega_{R_2^s} + \omega_{1,2^s}. \end{aligned}$$

Note that (K_0, ω_0) , (K_{R_1}, ω_{R_1}) , (K_{R_2}, ω_{R_2}) and $(K_{R_2^s}, \omega_{R_2^s})$ satisfy the dispersion relation for electromagnetic waves (2.15) while $(K_{1,1}, \omega_{1,1})$, $(K_{1,2}, \omega_{1,2})$ and

$(K_{1,2^s}, \omega_{1,2^s})$ satisfy the one for electron-plasma waves (2.14). That means that we have

$$\begin{aligned}\omega_{R_1} &= \sqrt{\omega_{pe}^2 + c^2(k_{R_1}^2 + \ell_{R_1}^2)}, \\ \omega_{R_2} &= \sqrt{\omega_{pe}^2 + c^2(k_{R_2}^2 + \ell_{R_2}^2)}, \\ \omega_{R_2^s} &= \sqrt{\omega_{pe}^2 + c^2(k_{R_2^s}^2 + \ell_{R_2^s}^2)}.\end{aligned}$$

Since K_2 and K_2^s are symmetric with respect to K_0 , choosing K_0 collinear to the x -axis, we have $k_{R_2} = k_{R_2^s}$ and $\ell_{R_2} = -\ell_{R_2^s}$. Therefore, one has $\omega_{R_2} = \omega_{R_2^s}$ and $\omega_{1,2} = \omega_{1,2^s}$. In the sequel, we replace $\omega_{R_2^s}$ and $\omega_{1,2^s}$ by respectively ω_{R_2} and $\omega_{1,2}$.

4.2 The equations.

As in Section 2, one gets the following set of equations, assuming that K_0 is collinear to the x -axis,

$$\begin{aligned}i\left(\partial_t + \frac{c^2}{\omega_0^2} K_0 \cdot \nabla\right) A_0 + \left(\frac{c^2 k_0^2}{2\omega_0^2} \Delta - \frac{c^4}{2\omega_0^4} (K_0 \cdot \nabla)^2\right) A_0 &= \frac{2\pi e^2}{m_e \omega_0} p A_0 \\ - \frac{e}{2m_e \omega_0} \nabla \cdot \mathbf{E}_{||} \left(A_{R_1} e^{-i\theta_{1,1}} \frac{K_0 \cdot K_{R_1}}{|K_0||K_{R_1}|} + A_{R_2} e^{-i\theta_{1,2}} \frac{K_0 \cdot K_{R_2}}{|K_0||K_{R_2}|} + A_{R_2^s} e^{-i\theta_{1,2^s}} \frac{K_0 \cdot K_{R_2^s}}{|K_0||K_{R_2^s}|} \right),\end{aligned}\quad (4.1)$$

$$\begin{aligned}i\left(\partial_t + \frac{c^2}{\omega_{R_1}} K_{R_1} \cdot \nabla\right) A_{R_1} + \frac{1}{2\omega_{R_1}} \left(c^2 \Delta - \frac{c^4}{\omega_{R_1}^2} (K_{R_1} \cdot \nabla)^2\right) A_{R_1} \\ = \frac{2\pi e^2}{m_e \omega_{R_1}} p A_{R_1} - \frac{e}{2m_e \omega_{R_1}} \nabla \cdot \mathbf{E}_{||}^* A_0 e^{i\theta_{1,1}} \frac{K_0 \cdot K_{R_1}}{|K_0||K_{R_1}|},\end{aligned}\quad (4.2)$$

$$\begin{aligned}i\left(\partial_t + \frac{c^2}{\omega_{R_2}} K_{R_2} \cdot \nabla\right) A_{R_2} + \frac{1}{2\omega_{R_2}} \left(c^2 \Delta - \frac{c^4}{\omega_{R_2}^2} (K_{R_2} \cdot \nabla)^2\right) A_{R_2} \\ = \frac{2\pi e^2}{m_e \omega_{R_2}} p A_{R_2} - \frac{e}{2m_e \omega_{R_2}} \nabla \cdot \mathbf{E}_{||}^* A_0 e^{i\theta_{1,2}} \frac{K_0 \cdot K_{R_2}}{|K_0||K_{R_2}|},\end{aligned}\quad (4.3)$$

$$\begin{aligned}i\left(\partial_t + \frac{c^2}{\omega_{R_2^s}} K_{R_2^s} \cdot \nabla\right) A_{R_2^s} + \frac{1}{2\omega_{R_2^s}} \left(c^2 \Delta - \frac{c^4}{\omega_{R_2^s}^2} (K_{R_2^s} \cdot \nabla)^2\right) A_{R_2^s} \\ = \frac{2\pi e^2}{m_e \omega_{R_2^s}} p A_{R_2^s} - \frac{e}{2m_e \omega_{R_2^s}} \nabla \cdot \mathbf{E}_{||}^* A_0 e^{i\theta_{1,2^s}} \frac{K_0 \cdot K_{R_2^s}}{|K_0||K_{R_2^s}|},\end{aligned}\quad (4.4)$$

$$\begin{aligned}i\partial_t \mathbf{E}_{||} + \frac{v_{th}^2}{2\omega_{pe}} \Delta \mathbf{E}_{||} = \frac{\omega_{pe}^2}{2} p \mathbf{E}_{||} + \frac{\omega_{pe} e}{2m_e c^2} \nabla \left(A_0 A_{R_1}^* e^{i\theta_{1,1}} \frac{K_0 \cdot K_{R_1}}{|K_0||K_{R_1}|} \right. \\ \left. + A_0 A_{R_2}^* e^{i\theta_{1,2}} \frac{K_0 \cdot K_{R_2}}{|K_0||K_{R_2}|} + A_0 A_{R_2^s}^* e^{i\theta_{1,2^s}} \frac{K_0 \cdot K_{R_2^s}}{|K_0||K_{R_2^s}|} \right),\end{aligned}\quad (4.5)$$

$$\left(\partial_t^2 - c_s^2 \Delta\right)p = \frac{1}{4\pi m_i} \Delta \left(|\mathbf{E}_{||}|^2 + \frac{\omega_{pe}^2}{c^2} (|A_0|^2 + |A_{R_1}|^2 + |A_{R_2}|^2 + |A_{R_2^s}|^2) \right). \quad (4.6)$$

Note that since the Raman components are not resonant one another, one gets two distinct equations without coupling terms like $A_{R_1} A_{R_2}^*$ and the same procedure as in Section 2 can be used. A non-dimensional form can be obtained. Using $\frac{1}{\omega_0}$ as time scale, $\frac{1}{|K_0|}$ as space scale and denoting

$$\begin{aligned} \tilde{A}_0 &= \sqrt{\omega_0} \frac{\omega_{pe}}{c} \frac{A_0}{\gamma}, \quad \tilde{A}_{R_1} = \sqrt{\omega_{R_1}} \frac{\omega_{pe}}{c} \frac{A_{R_1}}{\gamma}, \quad \tilde{A}_{R_2} = \sqrt{\omega_{R_2}} \frac{\omega_{pe}}{c} \frac{A_{R_2}}{\gamma}, \\ \tilde{A}_{R_2^s} &= \sqrt{\omega_{R_2}} \frac{\omega_{pe}}{c} \frac{A_{R_2^s}}{\gamma}, \quad \tilde{\mathbf{E}}_{||} = \frac{\sqrt{\omega_{pe}}}{\gamma} \mathbf{E}_{||}, \end{aligned}$$

with

$$\gamma = \frac{2m_e \omega_0}{ek_0} \sqrt{\omega_0 \omega_{pe} \omega_{R_1}},$$

we obtain (dropping the tildes) and recalling that

$$\alpha = \sqrt{\frac{\omega_{R_1}}{\omega_{R_2}}},$$

$$\begin{aligned} i \left(\partial_t + \frac{c^2 k_0^2}{\omega_0^2} \partial_x \right) A_0 + \left(\frac{c^2 k_0^2}{2\omega_0^2} \Delta - \frac{c^4 k_0^4}{2\omega_0^4} \partial_x^2 \right) A_0 &= \frac{\omega_{pe}^2}{2\omega_0^2} p A_0 \\ - \nabla \cdot \mathbf{E}_{||} \left(A_{R_1} e^{-i\theta_{1,1}} \frac{k_{R_1}}{|K_{R_1}|} + \alpha (A_{R_2} e^{-i\theta_{1,2}} + A_{R_2^s} e^{-i\theta_{1,2^s}}) \frac{k_{R_2}}{|K_{R_2}|} \right), \end{aligned} \quad (4.7)$$

$$\begin{aligned} i \left(\partial_t + \frac{c^2 k_0}{\omega_{R_1} \omega_0} K_{R_1} \cdot \nabla \right) A_{R_1} + \frac{1}{2\omega_{R_1} \omega_0} \left(c^2 k_0^2 \Delta - \frac{c^4 k_0^2}{\omega_{R_1}^2} (K_{R_1} \cdot \nabla)^2 \right) A_{R_1} \\ = \frac{\omega_{pe}^2}{2\omega_0 \omega_{R_1}} p A_{R_1} - \nabla \cdot \mathbf{E}_{||}^* A_0 e^{i\theta_{1,1}} \frac{k_{R_1}}{|K_{R_1}|}, \end{aligned} \quad (4.8)$$

$$\begin{aligned} i \left(\partial_t + \frac{c^2 k_0}{\omega_{R_2} \omega_0} K_{R_2} \cdot \nabla \right) A_{R_2} + \frac{1}{2\omega_{R_2} \omega_0} \left(c^2 k_0^2 \Delta - \frac{c^4 k_0^2}{\omega_{R_2}^2} (K_{R_2} \cdot \nabla)^2 \right) A_{R_2} \\ = \frac{\omega_{pe}^2}{2\omega_0 \omega_{R_2}} p A_{R_2} - \alpha \nabla \cdot \mathbf{E}_{||}^* A_0 e^{i\theta_{1,2}} \frac{k_{R_2}}{|K_{R_2}|}, \end{aligned} \quad (4.9)$$

$$\begin{aligned} i \left(\partial_t + \frac{c^2 k_0}{\omega_{R_2} \omega_0} K_{R_2^s} \cdot \nabla \right) A_{R_2^s} + \frac{1}{2\omega_{R_2} \omega_0} \left(c^2 k_0^2 \Delta - \frac{c^4 k_0^2}{\omega_{R_2}^2} (K_{R_2^s} \cdot \nabla)^2 \right) A_{R_2^s} \\ = \frac{\omega_{pe}^2}{2\omega_0 \omega_{R_2}} p A_{R_2^s} - \alpha \nabla \cdot \mathbf{E}_{||}^* A_0 e^{i\theta_{1,2^s}} \frac{k_{R_2}}{|K_{R_2}|}, \end{aligned} \quad (4.10)$$

$$\begin{aligned}
i\partial_t \mathbf{E}_{||} + \frac{v_{th}^2 k_0^2}{2\omega_{pe}\omega_0} \Delta \mathbf{E}_{||} &= \frac{\omega_{pe}}{2\omega_0} p \mathbf{E}_{||} + \nabla \left(A_0 A_{R_1}^* e^{i\theta_{1,1}} \frac{k_{R_1}}{|K_{R_1}|} \right. \\
&\left. + \alpha (A_0 A_{R_2}^* e^{i\theta_{1,2}} + A_0 A_{R_2^s}^* e^{i\theta_{1,2^s}}) \frac{k_{R_2}}{|K_{R_2}|} \right), \tag{4.11}
\end{aligned}$$

$$\begin{aligned}
(\partial_t^2 - c_s^2 \Delta) p &= \frac{4m_e}{m_i} \frac{\omega_0 \omega_{R_1}}{\omega_{pe}^2} \Delta \left(|\mathbf{E}_{||}|^2 + \frac{\omega_{pe}}{\omega_0} |A_0|^2 + \frac{\omega_{pe}}{\omega_{R_1}} |A_{R_1}|^2 \right. \\
&\left. + \frac{\omega_{pe}}{\omega_{R_2}} (|A_{R_2}|^2 + |A_{R_2^s}|^2) \right). \tag{4.12}
\end{aligned}$$

Remark 4.1. Note that the only new coefficient is the ratio of the Raman frequencies $\frac{\omega_{R_1}}{\omega_{R_2}}$.

5 Numerical simulations.

5.1 The scheme.

We adapt the scheme introduced in [8]. We consider a regular mesh in space. The fields are approximated by $A_{i,j}$ for $i = 0, \dots, N_x$ and $j = 0, \dots, N_y$. We use periodic boundary conditions that is for all $j = 0, \dots, N_y$, $A_{0,j} = A_{N_x,j}$. In space, we consider centered finite difference discretization for each differential operator. Introducing

$$\begin{aligned}
X_0^{n+1} &= \frac{A_0^{n+1} + A_0^n}{2}, \quad X_{R_1}^{n+1} = \frac{A_{R_1}^{n+1} + A_{R_1}^n}{2}, \quad X_{R_2}^{n+1} = \frac{A_{R_2}^{n+1} + A_{R_2}^n}{2}, \\
X_{R_2^s}^{n+1} &= \frac{A_{R_2^s}^{n+1} + A_{R_2^s}^n}{2}, \quad X_{\mathbf{E}^{n+1}} = \frac{\mathbf{E}^{n+1} + \mathbf{E}^n}{2}, \quad X_p^{n+1} = \frac{p^{n+1} + p^n}{2},
\end{aligned}$$

as new unknowns, the scheme reads

$$\begin{aligned}
2i \frac{X_0^{n+1} - A_0^n}{\Delta t} + i \frac{c^2 k_0^2}{\omega_0^2} \partial_x X_0^{n+1} + \left(\frac{c^2 k_0^2}{2\omega_0^2} \Delta - \frac{c^4 k_0^4}{2\omega_0^4} \partial_x^2 \right) X_0^{n+1} \\
= \frac{\omega_{pe}^2}{2\omega_0^2} X_p^{n+1} X_0^{n+1} - \frac{1}{2} \left(\Psi_{\mathbf{E}}^{n+\frac{1}{2}} X_{R_1}^{n+1} + \nabla \cdot X_{\mathbf{E}}^{N+1} \Phi_{A_{R_1}}^{n+\frac{1}{2}} \right) e^{-i\theta_{1,1}^{N+\frac{1}{2}}} \frac{k_{R_1}}{|K_{R_1}|} \\
- \frac{\alpha}{2} \left(\Psi_{\mathbf{E}}^{n+\frac{1}{2}} X_{R_2}^{n+1} + \nabla \cdot X_{\mathbf{E}}^{N+1} \Phi_{A_{R_2}}^{n+\frac{1}{2}} \right) e^{-i\theta_{1,2}^{N+\frac{1}{2}}} \frac{k_{R_2}}{|K_{R_2}|} \\
- \frac{\alpha}{2} \left(\Psi_{\mathbf{E}}^{n+\frac{1}{2}} X_{R_2^s}^{n+1} + \nabla \cdot X_{\mathbf{E}}^{N+1} \Phi_{A_{R_2^s}}^{n+\frac{1}{2}} \right) e^{-i\theta_{1,2^s}^{N+\frac{1}{2}}} \frac{k_{R_2}}{|K_{R_2}|}, \tag{5.1}
\end{aligned}$$

where

$$\begin{aligned}
\frac{\Psi_{\mathbf{E}}^{n+\frac{1}{2}} + \Psi_{\mathbf{E}}^{n-\frac{1}{2}}}{2} &= \nabla \cdot \mathbf{E}^n, \quad \frac{\Phi_{A_{R_1}}^{n+\frac{1}{2}} + \Phi_{A_{R_1}}^{n-\frac{1}{2}}}{2} = A_{R_1}^n, \\
\frac{\Phi_{A_{R_2}}^{n+\frac{1}{2}} + \Phi_{A_{R_2}}^{n-\frac{1}{2}}}{2} &= A_{R_2}^n, \quad \frac{\Phi_{A_{R_2^s}}^{n+\frac{1}{2}} + \Phi_{A_{R_2^s}}^{n-\frac{1}{2}}}{2} = A_{R_2^s}^n,
\end{aligned}$$

are auxiliary functions. The equations of System (4.8) – (4.12) are discretized in the following way

$$\begin{aligned}
& 2i \frac{X_{A_{R_1}}^{n+1} - A_{R_1}^n}{\Delta t} + \frac{c^2 k_0}{\omega_{R_1} \omega_0} K_{R_1} \cdot \nabla X_{R_1}^{n+1} + \frac{1}{2\omega_{R_1} \omega_0} \left(c^2 k_0^2 \Delta - \frac{c^4 k_0^2}{\omega_{R_1}^2} (K_{R_1} \cdot \nabla)^2 \right) X_{R_1}^{n+1} \\
& = \frac{\omega_{pe}^2}{2\omega_0 \omega_{R_1}} X_p^{n+1} X_{R_1}^{n+1} - \left(\Psi_{\mathbf{E}}^{n+\frac{1}{2}} \right)^* X_0^{n+1} e^{i\theta_{1,1}^{n+\frac{1}{2}}} \frac{k_{R_1}}{|K_{R_1}|}, \tag{5.2}
\end{aligned}$$

$$\begin{aligned}
& 2i \frac{X_{A_{R_2}}^{n+1} - A_{R_2}^n}{\Delta t} + \frac{c^2 k_0}{\omega_{R_2} \omega_0} K_{R_2} \cdot \nabla X_{R_2}^{n+1} + \frac{1}{2\omega_{R_2} \omega_0} \left(c^2 k_0^2 \Delta - \frac{c^4 k_0^2}{\omega_{R_2}^2} (K_{R_2} \cdot \nabla)^2 \right) X_{R_2}^{n+1} \\
& = \frac{\omega_{pe}^2}{2\omega_0 \omega_{R_2}} X_p^{n+1} X_{R_2}^{n+1} - \left(\Psi_{\mathbf{E}}^{n+\frac{1}{2}} \right)^* X_0^{n+1} e^{i\theta_{1,2}^{n+\frac{1}{2}}} \frac{k_{R_2}}{|K_{R_2}|}, \tag{5.3}
\end{aligned}$$

$$\begin{aligned}
& 2i \frac{X_{A_{R_2^s}}^{n+1} - A_{R_2^s}^n}{\Delta t} + \frac{c^2 k_0}{\omega_{R_2} \omega_0} K_{R_2^s} \cdot \nabla X_{R_2^s}^{n+1} + \frac{1}{2\omega_{R_2} \omega_0} \left(c^2 k_0^2 \Delta - \frac{c^4 k_0^2}{\omega_{R_2}^2} (K_{R_2} \cdot \nabla)^2 \right) X_{R_2^s}^{n+1} \\
& = \frac{\omega_{pe}^2}{2\omega_0 \omega_{R_2}} X_p^{n+1} X_{R_2^s}^{n+1} - \left(\Psi_{\mathbf{E}}^{n+\frac{1}{2}} \right)^* X_0^{n+1} e^{i\theta_{1,2^s}^{n+\frac{1}{2}}} \frac{k_{R_2}}{|K_{R_2}|}, \tag{5.4}
\end{aligned}$$

$$\begin{aligned}
& i \frac{X_{\mathbf{E}}^{n+1} - X_{\mathbf{E}}^n}{\Delta t} + \frac{v_{th}^2 k_0^2}{2\omega_{pe} \omega_0} \Delta X_{\mathbf{E}}^{n+1} = \frac{\omega_{pe}}{2\omega_0} X_p^{n+1} X_{\mathbf{E}}^{n+1} + \nabla \left(X_0^{n+1} (\Phi_{A_{R_1}}^{n+\frac{1}{2}})^* e^{i\theta_{1,1}^{n+\frac{1}{2}}} \frac{k_{R_1}}{|K_{R_1}|} \right. \\
& \left. + \alpha (X_0^{n+1} (\Phi_{A_{R_2}}^{n+\frac{1}{2}})^* e^{i\theta_{1,2}^{n+\frac{1}{2}}} + X_0^{n+1} (\Phi_{A_{R_2^s}}^{n+\frac{1}{2}})^* e^{i\theta_{1,2^s}^{n+\frac{1}{2}}}) \frac{k_{R_2}}{|K_{R_2}|} \right), \tag{5.5}
\end{aligned}$$

$$\begin{aligned}
& \frac{p^{n+1} - 2p^n + p^{n-1}}{\Delta t^2} - c_s^2 \Delta \left(\frac{p^{n+1} + p^{n-1}}{2} \right) = \frac{4m_e}{m_i} \frac{\omega_0 \omega_{R_1}}{\omega_{pe}^2} \Delta \left(|\mathbf{E}^n|^2 + \frac{\omega_{pe}}{\omega_0} |A_0^n|^2 \right. \\
& \left. + \frac{\omega_{pe}}{\omega_{R_1}} |A_{R_1}^n|^2 + \frac{\omega_{pe}}{\omega_{R_2}} (|A_{R_2}^n|^2 + |A_{R_2^s}^n|^2) \right). \tag{5.6}
\end{aligned}$$

The scheme is inspired from that of C. Besse [4] and B. Glassey [10].

5.2 The test case.

The values of the different parameters are the same as the ones used in [8] and we refer to [8] for a complete description. In particular, v_0 , v_{R_1} and v_{R_2} denotes respectively the propagation speeds of A_0 , A_{R_1} and A_{R_2} . We denote θ the angle between the wave vectors A_0 and A_{R_2} and by θ_{\max} the angle corresponding to the maximum amplification rate for the Raman component propagating in the forward direction. We work on a system in dimensionless form. The unit of length is $\frac{1}{k_0}$ and the unit in time is $\frac{1}{\omega_0}$. The spatial domain is $x \in [0, 300]$ and $y \in [0, 200]$. The number of discretization points in x is $N_x = 300$ and the one

in y is $N_y = 200$. We compute on a time interval $[0, T]$ with $T = 200$. The number of time steps is $N_t = 576$. The initial data for A_0 is of the form

$$A_0(0, \cdot) = \alpha e^{-\beta_x(x-\gamma_x)^2} e^{-\beta_y(y-\gamma_y)^2}.$$

• **Case 1:** We consider a collision test case. We take $\theta = \theta_{\max}$. We define $\alpha = 0.1$, $\beta_x = \frac{1}{1250}$, $\beta_y = \frac{1}{1800}$. The initial data for A_{R_1} and A_{R_2} are localized at different positions. Therefore, after some time, these components interact in the middle of the computational box. More precisely, the interaction takes place at the point $x = 100$, $y = 100$. Taking into account the propagation speed of the different fields, we introduce the following parameters

$$L_{R_1}^x = \frac{v_{R_1}}{v_0} * 50, \quad L_{R_2}^x = \frac{v_{R_2}}{v_0} * 50 * \cos(\theta), \quad L_{R_2}^y = 100 - L_{R_2}^x * \tan(\theta).$$

We take

$$\begin{cases} A_0(0, \cdot) = \alpha e^{-\beta_x(x-50)^2} e^{-\beta_y(y-100)^2}, \\ A_R^1 = \frac{\alpha}{100} e^{-\beta_x(x-(100+L_{R_1}^x))^2} e^{-\beta_y(y-100)^2}, \\ A_R^2 = \frac{\alpha}{100} e^{-\beta_x(x-(100-L_{R_2}^x))^2} e^{-\beta_y(y-L_{R_2}^y)^2}. \end{cases} \quad (5.7)$$

The initial conditions for \mathbf{E} and p are equal to 0. This case corresponds to the maximum amplification rate for the second Raman component that is $\theta = \theta_{\max}$.

• **Case 2:** We now let θ varying from $\frac{1}{6}\theta_{\max}$ to $\frac{4}{3}\theta_{\max}$ and we keep $L_{R_2}^y = 100 - L_{R_2}^x * \tan(\theta)$. The initial conditions are the same as the ones used for Case 1.

• **Case 3 :** We keep A_0 as in Case 1 and we set the Raman components to zero. We also take $p_0 = p_1 = 0$ and a non-zero initial value for E , for instance $E_x = E_y = A_0$.

5.3 Comments

For convenience, we have rescaled all the fields. For each component, the maximum of the modulus is equal to 100. In Figure 5, we can observe the very beginning of the interaction at time $t = 50$. The maximum of the amplitude of A_0 is still near its maximum whereas the ones for A_{R_1} and A_{R_2} are far from their maximum. In Figure 6, we have reached the impact point. The support of the different Gaussians are nearly equal and so the amplification process is maximal. The two Raman components are growing exponentially whereas the amplitude of the incident laser field is decreasing. It is of course in agreement with the conservation law coming from System (4.7) – (4.12) and preserved by our numerical scheme

$$\frac{d}{dt} \int_{\mathbb{R}^n} \left(2|A_0|^2 + |A_{R_1}|^2 + |A_{R_2}|^2 + |A_{R_2}^s|^2 + |\mathbf{E}|^2 \right) ds = 0.$$

In Figure 7, the interaction has stopped since the supports became disjoint. One can observe the effects of the dispersion on the fields.

In Figure 8, we have plotted the maximum of the fields A_{R_1} and A_{R_2} with respect to the parameter $\gamma = \frac{\theta}{\theta_{\max}}$. We can observe that the angle θ has no influence on the field A_{R_1} . The influence on A_{R_2} is of great interest. As expected, the maximum for A_{R_2} is achieved for $\gamma = 1$. Furthermore one can observe that the process is much more efficient for $\gamma = 1$ than for example $\gamma = \frac{1}{6}$. Indeed, the ratio between the two maximum of the amplitude is around 20 per cent, which means that the gain is considerable.

Note that the shapes of the curves of Figure 2 and Figure 8 are not the same although the maximum is reached at the same point. It is due to the fact that Figure 2 comes from a very basic analysis while Figure 8 takes into account all the complex phenomena involved in the Raman instability. For example the influence of the fluctuation of the density of electrons is crucial and it is not taken into account in the linear analysis developed in Section 3.2. However we would like to emphasize that we obtain the right angle leading to the maximum amplification rate. Moreover, the curve of Figure 8 is flat at the maximum. It is due to the fact that the pulse is not monochromatic and therefore even if we prescribe the angle at a value that is different from the one giving the maximum amplification rate, a larger region is involved. Geometrically, the critical value is also concerned and the amplification is larger than that predicted by the linear theory.

In Figure 9, one can observe that, even if we start from a zero initial data for the Raman components, A_{R_1} and A_{R_2} do not stay equal to zero. This is due to the coupling quasilinear terms involved in Equations (4.2) and (4.3). Indeed, A_0 plays the role of a pump-wave in (4.2)-(4.3) and then excite the two Raman components. In Figure 9, we do not have rescaled the fields. One can note that the maxima of the modulus of the Raman fields are very small compare to the one of the incident laser field. This is due to the fact that the interaction time corresponding to the superposition of the support of the different gaussians involved is very short.

Acknowledgments

We wish to express our deepest gratitude to the referees for their very useful comments and remarks.

References

- [1] R. Belaouar, T. Colin, G. Gallice and C. Galusinski. *Theoretical and numerical study of a quasilinear system describing Landau damping*. M2AN Math. Model. Numer. Anal., Vol. 40(6), (2006), 961-990.
- [2] T.B. Benjamin, J.L. Bona and J.J. Mahony. *Model equations for long waves in nonlinear dispersive systems*. Philos. Trans. Roy. Soc. London Ser. A, Vol. 272(1220), (1972), 47-78
- [3] R.L. Berger, C.H. Still, A. Williams and A.B. Langdon. *On the dominant and subdominant behaviour of stimulated Raman and Brillouin scattering*. J. Plasma Physics, Vol. 12(1), (1974), 1-12

- louis scattering driven by nonuniform laser beams.* Physics of Plasma, Vol. 5, number 12, (1998), 4337-4356.
- [4] C. Besse. *Schéma de relaxation pour l'équation de Schrödinger non linéaire et les systèmes de Davey et Stewartson.* C.R. Acad. Sci. Paris. Sér. I Math., Vol. 326, (1998), 1427-1432.
- [5] J. Bona, H. Chen, S.M. Sun, B.-Y. Zhang, *Comparison of quarter-plane and two-point boundary value problems: the BBM-equation.* Discrete Contin. Dyn. Syst. 13 (2005), no. 4, 921–940.
- [6] R. Carles. *Geometric optics and instability for semi-linear Schrödinger equations.* Arch. Ration. Mech. Anal. 183, (2007), 525-553.
- [7] M. Colin and T. Colin. *On a quasi-linear Zakharov system describing laser-plasma interactions.* Diff. Int. Eqs, Vol. 17, 3-4, (2004), 297-330.
- [8] M. Colin and T. Colin. *A numerical model for the Raman amplification for laser-plasma interactions.* J. Comput. App. Math., Vol. **193**, 2, (2006), 535-562.
- [9] C.D. Decker, W.B. Mori, T. Katsouleas and D.E. Hinkel. *Spatial temporal theory of Raman forward scattering.* Physics of Plasma, Vol. 3, (1996), 1360-1372.
- [10] R.T. Glassey. *Convergence of an energy-preserving scheme for the Zakharov equation in one space dimension.* Math. of Comput. Vol. 58, Number 197, (1992), 83-102.
- [11] N. Hayashi, P.I. Naumkin, P-N. Pipolo, *Smoothing effects for some derivative nonlinear Schrödinger equations,* Discrete Contin. Dynam. Systems 5 (1999), no. 3, 685–695.
- [12] W.L. Kruer. *The physics of laser plasma interactions.* New York : Addison-Wesley, (1988).
- [13] K. Barrailh, D. Lannes, *A general framework for diffractive optics and its applications to lasers with large spectrums and short pulses,* SIAM J. Math. Anal. 34 (2002), no. 3, 636–674.
- [14] R. Sentis, *Mathematical models for laser-plasma interaction.* M2AN Math. Model. Numer. Anal. 39 (2005), no. 2, 275–318.
- [15] M. Doumika, F. Duboc, F. Golse, and R. Sentis, *Simulation of laser beam propagation with a paraxial model in a tilted frame,* Journal of Computational Physics, Volume 228, Issue 3, 20 February 2009, Pages 861-880
- [16] B. Texier, *Derivation of the Zakharov equations,* Arch. Ration. Mech. Anal., 184 (1), (2007), 121-183.

- [17] V.E. Zakharov, S.L. Musher and A.M. Rubenchik. *Hamiltonian approach to the description of nonlinear plasma phenomena*. Phys. Reports, Vol. 129, (1985), 285-366.

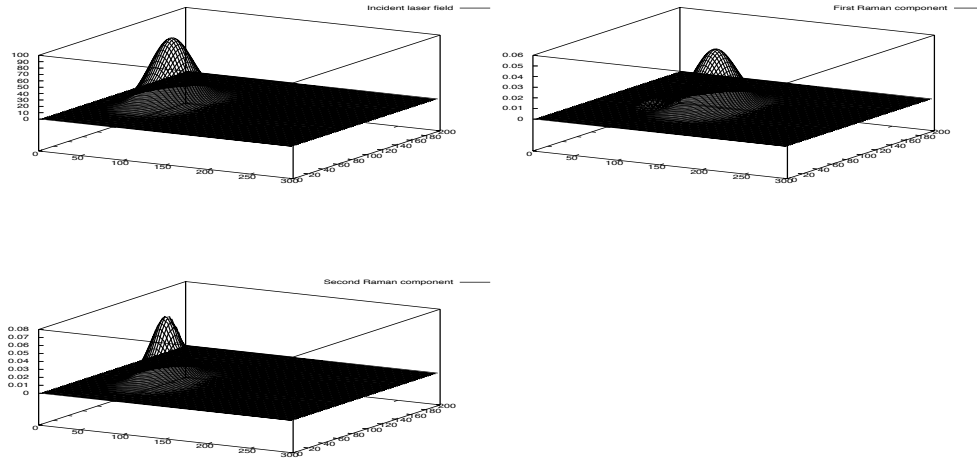


Figure 5: 2D-geometry, Case 1. Modulus of the rescaled fields at time $t=50$ with initial conditions (5.7). From left to right, first line A_0 and A_{R_1} , second line A_{R_2} .

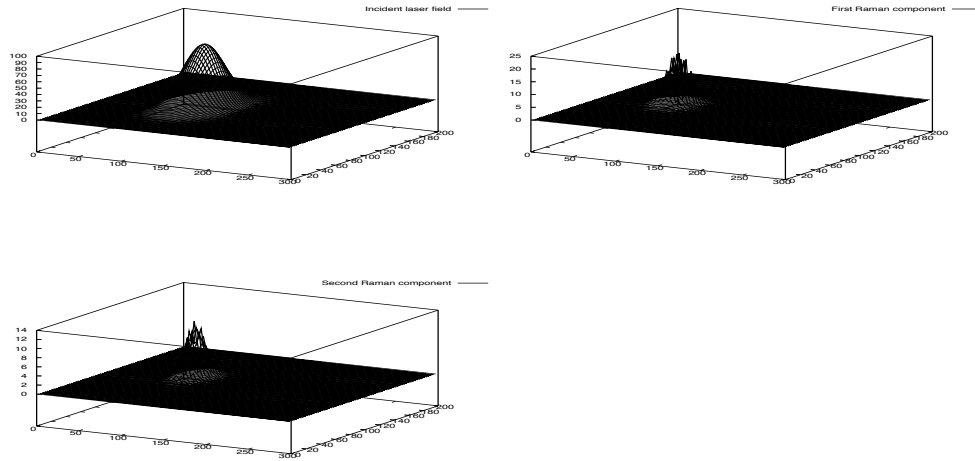


Figure 6: 2D-geometry, Case 1. Modulus of the rescaled fields at time $t=66$ with initial conditions (5.7). From left to right, first line A_0 and A_{R_1} , second line A_{R_2} .

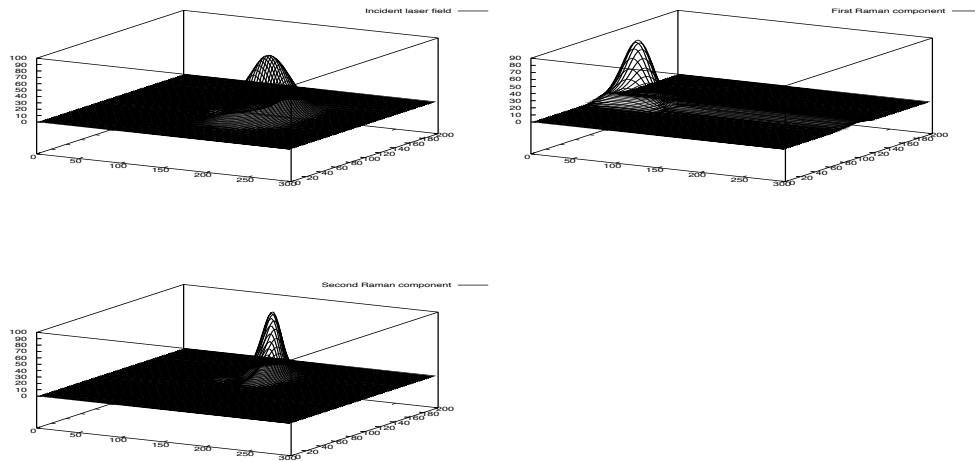


Figure 7: 2D-geometry, Case 1. Modulus of the rescaled fields at time $t=150$ with initial conditions (5.7). From left to right, first line A_0 and A_{R_1} , second line A_{R_2} .

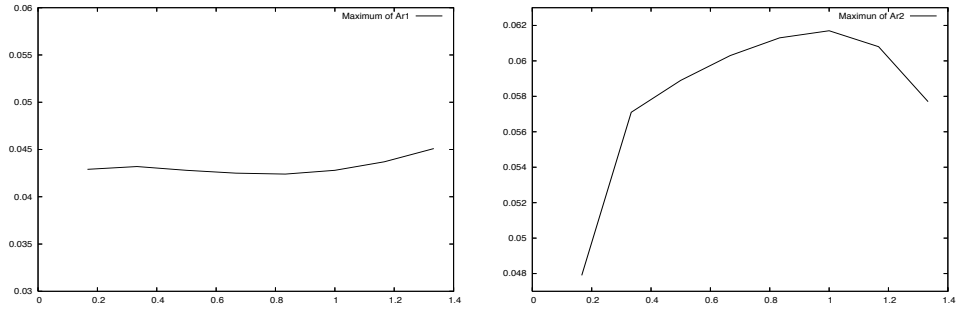


Figure 8: Case 2. Maximum of the fields with respect to the parameter $\gamma = \frac{\theta}{\theta_{\max}}$. We let gamma vary from $\frac{1}{6}$ to $\frac{8}{6}$. From left to right, A_{R_1} and A_{R_2} .

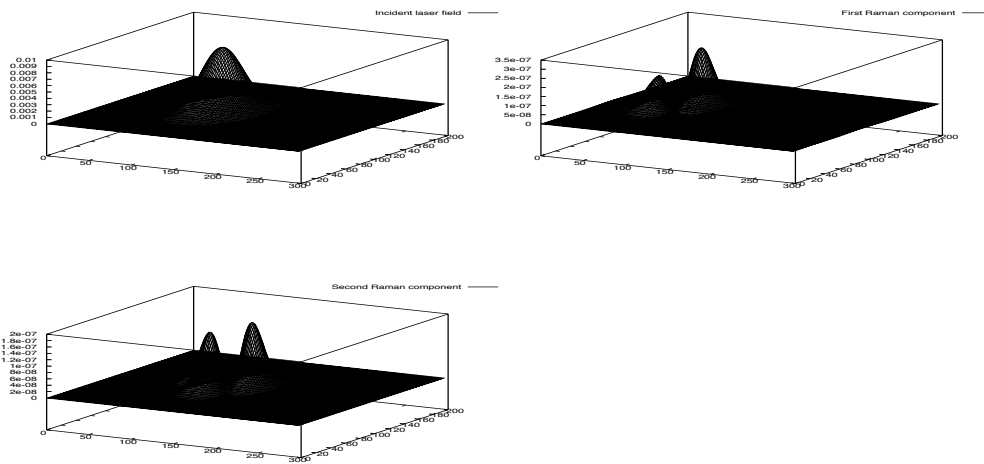


Figure 9: 2D-geometry, Case 3. Modulus of the fields at time $t=75$ with initial conditions (5.7). From left to right, first line A_0 and A_{R_1} , second line A_{R_2} .